

# NUCLEATION RATES OF WATER USING ADJUSTED SAFT-0 EOS

Fawaz Hrahsheh<sup>1</sup>

*Higher Colleges of Technology, ETS, MZWC, Abu Dhabi, 58855, UAE.*

*Al al-Bayt University, Department of Physics, Faculty of Science, Al-Mafraq, Jordan*

---

## Abstract

The SAFT-0 is an equation of state (EOS) that considers the effects of molecular association based on the statistical association fluid theory (SAFT). This EOS recently showed relatively successful calculations of the phase-equilibrium properties and the classical and nonclassical nucleation rates of methanol. Motivated by methanol results, we use the SAFT-0 EOS for water, in particular within the temperature range of anomalous density behavior below  $T_{max} = 277.15K$ . To do so, we adjust the effective temperature-dependent segment diameter in terms of the association energy in a way that the SAFT-0 EOS reproduces the water vapor-liquid equilibria and the vapor pressures, particularly in the temperature range where the data of nucleation rates of water are available (220-260 K). The Gibbsian form of classical nucleation theory (CNT) (known as the P-form) and nonclassical gradient theory (GT) calculations were carried out using the SAFT-0 EOS with and without including this adjusted diameter. Calculated rates were compared to the experimental values of Wölk and Strey [*J. Phys. Chem. B* 2001, **105**, 11683-11701]. In addition to the phase-equilibrium properties, this adjustment improved the nucleation rates from both GT and CNT by factors of 500 and 100, respectively. To explore this further, the GT and experimental rates were analyzed using Hale's scaled model [*J. Chem. Phys.*, 2005, **122**, 204509]. This analysis shows that the predictions of GT scale rela-

---

<sup>1</sup>fyh44f@mst.edu

tively well with those of the experimental data.

*Keywords:* Phase Equilibria, Nucleation, SAFT EOS, Hydrogen Bonding, Gradient Theory, Binodal Lines

---

## 1. Introduction

First-order phase transitions play an important role in nature as well as in many technical applications. Simple examples of first order phase transition are condensation[1], evaporation[2], crystallization[3, 4], and melting[5]. Such phase transitions have an energy barrier equal to the work of formation of a small embryo (or nucleus) of the new phase, which emerges from fluctuations within the "supersaturated" mother phase. This initiating process of most first-order phase transitions is called nucleation[6, 7]. The hallmark of such a transition is the discontinuous change of density, for example, the condensation of supersaturated vapor into liquid droplets. The first treatment of the thermodynamics of nucleation is due to Gibbs[8]. Gibbs showed that the reversible work required to form a nucleus of the new phase consists of two terms: a bulk (volumetric) term and a surface term.

Theoretical analysis of nucleation rates is of great importance in connection with atmospheric aerosol formation and materials synthesis, clustering and condensation in vapors, crystallization of liquid alloys, phase separation in solid solutions, kinetics of colloidal and biological systems and many other growth-related phenomena such as thin film condensation, epitaxy of semiconductor quantum dots and freestanding nanowires[9, 10, 11, 12].

One of the simplest examples to illustrate the mechanism of nucleation is the formation of a small liquid droplet in a supersaturated vapor[13]. If we compress a vapor at constant temperature, the condensation will not commence at the saturation pressure, but above it: the vapor remains in a metastable state for some time until thermal fluctuations form a sufficiently large cluster

or nucleus, which can grow spontaneously. Central to nucleation theory is the expression for the nucleus (critical-size nanodroplet for spontaneous growing) work of formation. In the 1870s Gibbs [8] showed that this reversible work equals the difference between the free energy of the metastable phase with and without the droplet present. This macroscopic change of free energy associated with the formation of a nucleus consisting of monomers always contains a volume term and a surface energy term.

Classical nucleation theory originated with the work of Volmer and Weber [14] in 1926. By using the kinetic theory of gases and equilibrium thermodynamics, they derived an expression for the nucleation rates. Farkas [15] (1927), Becker-Döring [16] (1935), Frenkel [17] (1939) and Zeldovich [18] (1942) established the steady-state version of the so-called classical nucleation theory (CNT). The CNT considers the droplet as a uniform bulk phase separated by a sharp interface from the old phase (metastable vapor). The distinct feature of this theory is that it needs experimentally accessible bulk thermodynamic properties to calculate the nucleation rates.

Calculations of the nucleation rate  $J$  are based on the so-called Becker-Döring [16] expression. They assumed that during nucleation, a cluster grows by gaining a molecule at a rate known as the nucleation (or condensation) rate. However, most experiments show that the classically calculated nucleation rates have an incorrect temperature dependence and poor agreement with experimental data [19, 20, 21]. Nonclassical nucleation theories using the density functional theory (DFT) [22] and the gradient theory (GT) [23, 24, 25, 26, 27, 28, 29, 30], an approximation of DFT, predict a  $T$ -dependence in good agreement with experiment. Instead of the sharp discontinuity of density in the classical nucleation theory (CNT), DFT and GT treat the droplet as a non-uniform system whose density varies continuously with distance from the center of the droplet, eventually reaching the value of the surrounding mother phase.

Nucleation, as the first stage, determines many important properties of the newly forming phase such as the number density, and the size distribution of the nuclei [31, 32]. We need to understand the nucleation process in order to

control these parameters in experiments or technical applications. For instance, the number and size of nucleating water droplets has an impact on the efficiency and lifetime of a steam turbine as well as the color and reflectivity of clouds, which in turn influence the greenhouse effect. Nucleation of water is perhaps the most popular example in the literature, due to its relevance to industry; in boilers or turbines, in biological systems, or in atmospheric sciences and climate modeling[11]. A previous calculation applied to water using the cubic perturbed hard body (CPHB) with the  $P$ -form of CNT improved the predicted nucleation rate values by several orders of magnitudes compared to the conventional CNT, but it failed to improve the predicted temperature dependence of the rates [30]. The results of another calculation applied to methanol using the statistical association fluid theory SAFT-0 EOS [33] with the GT and the  $P$ -form of CNT [34, 35] have motivated us to extend the study to water. The semi-empirical Hale model [36, 37, 38] of nucleation rate shows that the methanol rate data exhibit anomalous  $S - T$  dependence while the GT rates using SAFT-0 EOS scale remarkably well, illustrating that the Hale plot can be used to assess the theoretical results and the experimental data, as well.

Despite several extensions and theoretical advances, classical nucleation theory (CNT) is still the most widely used theoretical tool used to predict nucleation rates[39, 40, 41, 42]. Since the popular classical nucleation theory (CNT) deviates by orders of magnitude from experiments for most substances[43], Wilhelmson et. al.[23, 44] investigated whether part of this discrepancy can be accounted for by the curvature-dependence of the surface tension. To that end, they evaluated the leading order corrections for water, the Tolman length and the rigidity constants, using square gradient theory coupled with the accurate CPA (Cubic-Plus-Association) equation of state[45, 46]. The Helfrich expansion[47] is then used to incorporate the curvature corrections into the CNT-framework. For water, this curvature-corrected CNT corrects the wrong temperature dependence of the nucleation rates given by the traditional CNT. Because the CPA equation of state does not reproduce the experimental water data below the temperature of maximum density[48] ( $T_{max} \simeq 277.15K$ ), they

applied a linear extrapolation to obtain the coefficients in the Helfrich expansion for water below this temperature where many of the nucleation experiments for water have been performed.

Similar to CPA EOS, the SAFT-0 is cubic and accurate equation of state, thus it is convenient to use it with the gradient theory to calculate the nucleation rates of non-polar and polar compounds, especially water. In this paper, we adjust the prerequisites of the SAFT-0 EOS itself in a way that it reproduces the vapor pressures and the anomalous water binodal lines below  $T_{max} = 277.15K$  in a good agreement with the experimental data [49]. Moreover, we apply the GT and CNT to water using SAFT-0 EOS to see if this adjustment will yield improved rates predictions in the temperature range where most of the nucleation rates were measured [20, 50]. It is imperative to mention that the difference between our work and Wilhelmsen et. al. is that we aim to improve the calculated nucleation rates of water by adjusting the SAFT-0 EOS itself, whereas they do so by incorporating the curvature dependence of the surface tension in the CNT. Interestingly, our results support their work very well. The distinct advantage of adjusting the SAFT-0 EOS itself is the simplicity and flexibility of applying it on more complex systems, particularly the aqueous binary and ternary mixtures below  $T_{max}$ , using the regular mixing rules. Also, adjusting the temperature dependent segment diameter, only, keeps the predictivity and cubicity of SAFT-0 EOS.

## 2. Theory and Computational Approaches

The reversible work  $W$  needed to create a critical-size cluster of the new phase in a metastable vapor is given by Gibbs [8] as:

$$W = A\gamma - V(P_l - P_v). \quad (1)$$

Here,  $A$  and  $\gamma$  are the surface area and surface tension, respectively, of the cluster,  $V$  is its volume,  $P_l$  and  $P_v$  are the internal pressure of the new bulk reference phase and the actual pressure of the mother phase, respectively, at

the same value of the chemical potential for both phases. Using the Laplace equation for the pressure difference between two phases separated by a curved surface, Gibbs [8] found an explicit relation for the work of formation  $W$  of critical size droplet as:

$$W = \frac{16\pi}{3} \frac{\gamma_\infty^3}{(P_l - P_v)^2}. \quad (2)$$

Here, the curved surface tension  $\gamma$  is approximated by the experimentally reachable values of flat interfaces  $\gamma_\infty$  because of a lack of knowledge of the exact surface tension  $\gamma$  for typical critical droplets (one nanometer or less radii). Obeidat et al. [34, 30] called Eqn.2 the  $P$ -form of work of formation. Gibbs' method for calculating the pressure  $P_l$  will be described below.

Calculating the accurate work of formation of the critical-size droplets is the challenge to use the Becker-Döring [16] expression of nucleation rate at a specific temperature  $T$ ,

$$J = J_0 \exp\left(-\frac{W}{k_B T}\right), \quad (3)$$

where  $k_B$  is Boltzmann constant, and the pre-exponential factor  $J_0$  is given as [30]:

$$J_0 = \sqrt{\frac{2\gamma_\infty}{\pi m_v}} v_l \left(\frac{P_v}{k_B T}\right)^2, \quad (4)$$

where  $m_v$  is the mass of a condensible vapor molecule, and  $v_l$  is the molecular volume of the new phase.

The Gibbs' expression of the reversible work (Eqn. 1) contains two terms: a bulk or volumetric term that thermodynamically stabilizes the droplet, and a surface term that is destabilizing because of the increase of free energy associated with forming new surface. Since the surface term is crucial for using Becker-Döring model of nucleation, Cahn and Hilliard [26] wrote the Helmholtz free energy  $F$  as a functional of the system density  $\rho$  with the square-gradient approximation, first proposed by van der Waals [25], to account for the inhomogeneous interfacial region separating the critical droplet from the uniform

mother phase. Their functional is given by:

$$F[\rho(r)] = \int dr f[\rho(r)] = \int dr (f_0[\rho(r)] + (c/2)[\nabla\rho(r)]^2). \quad (5)$$

Here,  $f$  and  $f_0$  are the Helmholtz free energy densities of the inhomogeneous and homogeneous fluids, respectively, and  $c$  is the so-called influence parameter [51], which is evaluated as a function of temperature by forcing agreement between calculated and experimental values of the bulk surface tension. The equilibrium droplet density profile that makes the work of formation an extreme value can be found by solving the following Euler-Lagrange equation:

$$\mu = \mu_0 - c\nabla^2\rho(r) \quad (6)$$

where  $\mu$  and  $\mu_0(\rho)$  are the chemical potentials of the bulk vapor phase and the homogeneous fluid, respectively, at density  $\rho$ . Expressions for  $f_0$  and  $\mu_0$  are readily found from a given equation of state.

Cahn and Hilliard first found the reversible work of critical nucleus formation can be evaluated as:

$$W = \int [\Delta W + (c/2)(\nabla\rho)^2]dV, \quad (7)$$

where  $\Delta W = W(\rho) - W(\rho_v)$ ,  $W(\rho) = f_0 - \rho\mu$ , and  $\rho$  is the density of the bulk phase. This work of formation may be used in Equation (3) to determine the nucleation rates. Obeidat, Li and Wilemski[30, 35, 51, 52] provide a comprehensive explanation of implementing the GT to calculate the work of formation of critical nanodroplets. In this work we exactly follow their steps but with the adjusted SAFT-0 EOS.

To calculate the binodal points, we derive the functional pressure and chemical potential from the Helmholtz free energy  $F$  as:

$$P(\rho) = \rho^2 \left( \frac{\partial F}{\partial \rho} \right)_T \quad (8)$$

$$\mu(\rho) = \rho \left( \frac{\partial F}{\partial \rho} \right)_T + F(\rho). \quad (9)$$

Then we determine the coexisting densities of bulk liquid  $\rho_{le}$  and vapor  $\rho_{ve}$  by solving the simultaneous equations

$$P(T, \rho_{le}) = P(T, \rho_{ve}), \quad (10)$$

$$\mu(T, \rho_{le}) = \mu(T, \rho_{ve}), \quad (11)$$

where  $\rho_{le}$  and  $\rho_{ve}$  are the equilibrium vapor and liquid densities, respectively. Gibbs' assumed the temperature and chemical potential are the same everywhere in the nonuniform system[8], i.e.,  $\mu(T, \rho_v) = \mu(T, \rho_l)$ . After subtracting the equilibrium value of chemical potential from both sides of this equation, we obtain

$$\mu(T, \rho_l) - \mu(T, \rho_{le}) = \mu(T, \rho_v) - \mu(T, \rho_{ve}). \quad (12)$$

Once  $\rho_l$  has been found by solving Eq.12, the reference pressure  $P(T, \rho_l)$  (pressure inside the droplet) is straightforward to calculate from EOS.

### 3. Adjusted SAFT EOS

The application of perturbation theory to associating systems in an equation of state was not practical until Wertheim developed his multi-density statistical mechanics for associating fluids[53]. Perturbation theories based on Wertheim's multi-density statistical mechanics have come to be called thermodynamic perturbation theory (TPT). In TPT, there is two energy scales: a short ranged highly directional association energy scale (hydrogen bonding energy scale) and an orientationally averaged (non- association) energy scale (reference energy scale). Typically, the reference energy scale accounts for dispersion attractions, dipolar attractions not accounted for through the association term and higher order multi-pole contributions. Thermodynamic perturbation theory (TPT) forms the basis of the statistical associating fluid theory (SAFT) family of equations of state[33, 54, 55, 56]. Chapman, et al. [33] proposed the first equation of

state based on the statistical associating fluid theory (SAFT). They wrote the Helmholtz molar free energy  $F$  as:

$$F = F^{id} + F^{seg} + F^{chain} + F^{assoc} \quad (13)$$

where  $F^{id}$ ,  $F^{seg}$ ,  $F^{chain}$  and  $F^{assoc}$  are the ideal term, the segment term, the chain term and the association term, respectively. It is now referred to as SAFT-0 [57] and we briefly summarized it in a previous work ([35]). While traditional cubic EOSs such as PR and SRK only have a single energy scale of attraction, SAFT allows for separate accounting of hydrogen bonding and reference (non-hydrogen bonding) attraction degrees of freedom. The strength of SAFT-0 EOS emerges from the association term  $F^{assoc}$  for self-associating compounds which is given by:

$$\frac{F^{assoc}}{RT} = \sum_{A=A,B,\dots} \left( \ln X^A - \frac{X^A}{2} \right) + \frac{1}{2M} \quad (14)$$

where  $R$  is the universal gas constant,  $M$  is the total number of association sites on each molecule,  $X^A$  is the mole fraction of molecules not bonded at site  $A$ , and  $\sum_A$  represents a sum over all associating sites on the molecule. Example for molecules with two attractive sites  $A$  and  $B$  (two-site model will be used below) is given as:

$$\frac{F^{assoc}}{RT} = \left( \ln X^A - \frac{X^A}{2} \right) + \left( \ln X^B - \frac{X^B}{2} \right) + \frac{1}{2}. \quad (15)$$

The mole fraction of molecules not bonded at sites  $A$  and  $B$  can, respectively, be calculated as follows:

$$X^A = \left[ 1 + N_{Av} \sum_{B=A,B} \rho X^B \Delta^{AB} \right]^{-1} \quad (16)$$

$$X^B = \left[ 1 + N_{Av} \sum_{A=A,B} \rho X^A \Delta^{BA} \right]^{-1} \quad (17)$$

where  $N_{Av}$  is the Avogadro's number, and  $\rho$  is the molar density of molecules, and  $\Delta^{AB}(\Delta^{BA})$  is the association strength, given as:

$$\Delta^{AB} = d^3 \left[ \frac{2 - \eta}{2(1 - \eta)^3} \right] \kappa^{AB} \left[ \exp \left( \frac{\epsilon^{AB}}{k_B T} - 1 \right) \right]. \quad (18)$$

Here,  $d$  is the effective temperature-dependent segment diameter,  $\kappa^{AB}$  is the dimensionless association volume,  $\epsilon^{AB}$  is the association energy, and  $\eta = \frac{\pi N_{Av}}{6} \rho d^3 m$  is the segment packing fraction.

The association sites in water can be represented by three different models: four-site model ( $M = 4$ ), three-site model ( $M = 3$ ), and two-site model ( $M = 2$ ). Suresh et. al. [58] evaluated these models by Wertheim’s thermodynamic perturbation theory (TPT) [53, 59]. They showed that any of the models may be accurately applied but they recommended the two-site model because its accuracy is at least equivalent to that of the other models and it is more convenient to apply in general. Taking into account the results of Wertheim’s TPT and the recommendation of Suresh et. al., Gross and Sadowski used the two-site model to apply the PC-SAFT EOS on water[55]. Here, we keep with this choice and the two-site model of water ( $M = 2$ ) will be used in this work.

The temperature-independent hard sphere diameter  $\sigma$  was related, following the Barcker-Henderson theory [60], to an effective temperature-dependent segment diameter,  $d(T_r, m)$  as [33]:

$$d(T_r, m) = \sigma f(T_r, m). \quad (19)$$

Here,  $f(T_r, m)$  is a generic function of the reduced temperature ( $T_r = \frac{K_B T}{\epsilon}$ ) by the Lennard-Jones intermolecular energy parameter  $\epsilon$ ,  $m$  is the number of segments per molecule, and  $\sigma$  is the temperature-independent hard sphere diameter. Barker and Henderson[60] introduced a temperature dependent form for  $d$  as

$$d = \sigma \int_0^1 \left[ 1 - \exp\left(\frac{-u(z)}{k_B T}\right) \right] dz, \quad (20)$$

where  $u(z)$  is the Lennard-Jones potential and  $z$  is the center-to-center distance between interacting (nonbonded) segments. Cotterman et. al. [61] numerically solved this integral for several temperatures and they determined an empirical formula for  $d$  by fitting its values for the spherical Lennard-Jones molecules as a function of reduced temperature  $T_r$ :

$$d(T_r, m) = \sigma \left[ \frac{1 + 0.2977T_r}{1 + 0.33163T_r + f(m)T_r^2} \right], \quad (21)$$

where  $f(m) = 0.0010477 + 0.025337(m - 1)/m$  is just an abbreviation in terms of  $m$ . For SAFT-0 EOS, Chapman et. al. [33] used the same empirical formula obtained by Cotterman et. al. for the Lennard-Jones potential. Although  $d(T_r, m)$  does not heavily change with  $T$ , it still can have a strong effect on the thermodynamics of the system, hence on the curves of the liquid-vapor coexistence.

It is known that water is highly polarized in the liquid state. Through detailed first principles quantum mechanics calculations for small water clusters[62], it has been shown that water hydrogen bond energy, polarization, and dipole moment[63, 64] depend on the number of times the water molecule is hydrogen bonded, as well as the type of hydrogen bonded cluster. Hence, there are both hydrogen bond cooperativity and cooperativity between the hydrogen bonding and the non-hydrogen bonding (reference) energy scales. Logically, this means that the reference energy in TPT should depend on the degree of hydrogen bonding[65, 66]. Marshall[65] have proposed a methodology to couple the reference energy scale to the degree of hydrogen bonding in the fluid with  $d = \sigma$ . Applying this methodology on water gave improved predictions of water-hydrocarbon mutual solubilities above  $T_{max}$ , but it did not improve the predictions of the pure water density or pressure. Later, Marshall[66] developed a second order thermodynamics perturbation theory (TPT2) to include hydrogen bond cooperativity for the case where a water molecule is a donor and a acceptor, at the same time. Also, as is common in perturbation theories, TPT2 with PC-SAFT and  $d = \sigma$  did not reproduce the density maximum of water. Replacing  $\sigma$  with  $d(T) < \sigma$  in the hard sphere contributions has the effect of increasing density as compared to the case where the hard sphere diameter  $\sigma$  was used in these contributions. Therefore, Marshall described the reason of using  $d = \sigma$  for water as following: Using  $d(T) < \sigma$  increases the average number of hydrogen bonds per water molecules with a decrease in temperature which results in the shortening of the hydrogen bonds. Marshall attributed the failure of predicting the water density maximum to that the density maximum is a result of the change in the water structure (hydrogen bonds number and length),

while TPT2 addressed only energetics.

Recently, Held et al.[67], Cameretti et al.[68], Cameretti[69] reported that accurate modeling of liquid densities of water cannot be obtained without modification of its temperature-dependent segment diameter. To do so, we take the exponential form of the temperature-dependent effective diameter in Chen and Kreglewski work [70] where the Barker-Henderson integral equation [71] was solved using a square-well potential as a suggestion to use exponential form for our desired adjustment. This exponential form is also supported by Held et al.[67] where they added a temperature-dependent exponential term to the temperature-independent hard sphere diameter  $\sigma$  in ePC-SAFT EOS[68] to treat the deviation of calculated water density between 273.15K and 373.15K. Later, Pereda et al.[72] studied the temperature dependence of the hydrocarbon solubility in water using the group contribution with association equation of state (GCA-EOS)[73, 74]. As a result of their study, they concluded that the temperature-dependent effective diameter  $d$  of water has a strong influence on the temperature dependence of the hydrocarbon solubility in water. Therefore, they introduced an exponential correction to  $d$  to improve the predictions of water-hydrocarbons mutual solubility within the temperature range 298 – 353K of their experimental data.

In the present work, we aim to couple the additive hydrogen bonding energy scale and the reference energy scale by including the association energy  $\epsilon^{AB}$  in the calculations of the effective temperature-dependent segment diameter. Then, we just need to find a way of adjusting  $d$  in terms of  $\epsilon^{AB}$  and  $T$  so that the SAFT-0 EOS successfully reproduces the water densities and the vapor pressures, particularly for  $T < T_{max} = 277.15K$ . Because the SAFT-0 EOS with the Cotterman’s form of  $d$  successfully predicts the water binodal line for  $T > T_{max}$  (with small deviations in the vicinity of  $T_{max}$ ) whereas it overpredicts it below  $T_{max}$ , we propose two conditions for the desired adjustment: It should quickly vanish above  $T_{max}$  and it should quickly increase below it. To apply these conditions in adjusting  $d$  with the site-site association energy, we introduce an exponential correction in terms of the dimensionless distance of

Table 1: Fitting parameters of SAFT-0 EOS for two-site water.

$\sigma$ [Å]	$\varepsilon/k_B$ [K]	$m$	$\epsilon^{AB}/k_B$ [K]	$\kappa^{AB}$
2.925	294.1	1.026	2938.8	0.053

the temperature from the water maximum density temperature  $\frac{T-T_{max}}{T_{max}}$  and the scaled association energy  $\frac{\epsilon^{AB}}{k_B T_{max}}$ . This correction is exclusive for water and the adjusted temperature-dependent segment diameter in SAFT-0 EOS becomes

$$d'(T_r, m) = d(T_r, m) + \sigma \lambda \exp \left[ -\frac{2}{3} \frac{\epsilon^{AB}}{k_B T_{max}} \left( \frac{T - T_{max}}{T_{max}} \right) \right]. \quad (22)$$

Here,  $\lambda\sigma = 0.02355$  is the correction at  $T_{max}$  where we calculate it by iteratively adding small corrections to  $d$  until we successfully reach the corresponding water experimental density (the maximum density). The liquid water’s anomalous behavior due to hydrogen bonding effect is accounted for by employing  $\frac{T-T_{max}}{T_{max}}$  to make the adjustment solely influential below  $T_{max}$ . The adjusted temperature-dependent segment diameter is bounded by  $T = 203 \pm 5K$  where a minimum density is evident there[75]. As far as we know, adjusting the temperature-dependent hard sphere diameter have never been made by including the association energy. We already tested this adjustment for four-site ( $M = 4$ ) model of water in a different subject of study that will be published in the near future.

In this paper, we apply the CNT ([35, 30]) and GT ([51, 35]) to calculate the nucleation rates of water using the adjusted SAFT-0 EOS. Its parameters for water (given in Table 1) are obtained by simultaneously fitting the experimental saturated vapor pressures and liquid densities [49].

#### 4. Results and Discussions

The effect of the adjustment on the temperature-dependent segment diameter is shown in Figure 1. The fast increase of  $d'$ , compared to  $d$ , as  $T$  drops down is the distinct feature of this adjustment. Specifically, this exponential increase of  $d'$  enables the SAFT-0 EOS to calculate the anomalous behavior

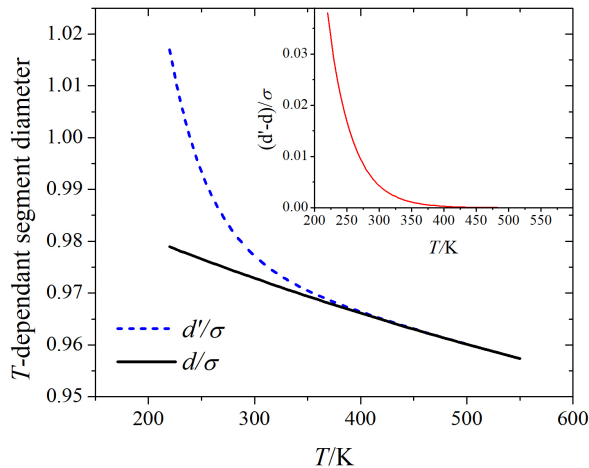


Figure 1: Comparison between the temperature-dependent segment diameter  $d$  (solid line) and the adjusted one  $d'$  (dashed line). Inset: The differences between these two diameters represent the adjustment term vs. temperature.

of the supercooled water density below  $T_{max}$  where the larger adjustment (as shown in the inset), the larger decrease in the liquid water density.

The predictions of SAFT-0 for the equilibrium vapor-liquid densities of water compared to the values calculated with the IAPWS-95 formulation [49] are shown in Figure 2 for several temperatures. IAPWS-95 is an analytical equation based on a multiparameter fit of all the experimental data available at temperatures above  $234K$  [49, 30]. Note that the results of the IAPWS-95 EOS may be regarded as the experimental values since this equation accurately treats the anomalous compressibility of supercooled liquid water and describes it to high precision above  $234K$ . Starting with the results of regular SAFT-0 EOS, we see that this equation accurately predicts the equilibrium vapor-liquid densities for  $T > 335K$ , but it is severely deficient in predicting the anomalous liquid binodal line below  $T_{max}$  (dashed line). Later, we will see the effect of this misprediction on calculating the nucleation rates of water. The adjusted SAFT-0 EOS fairly resolves this inaccuracy and predicts the binodal points (solid lines)

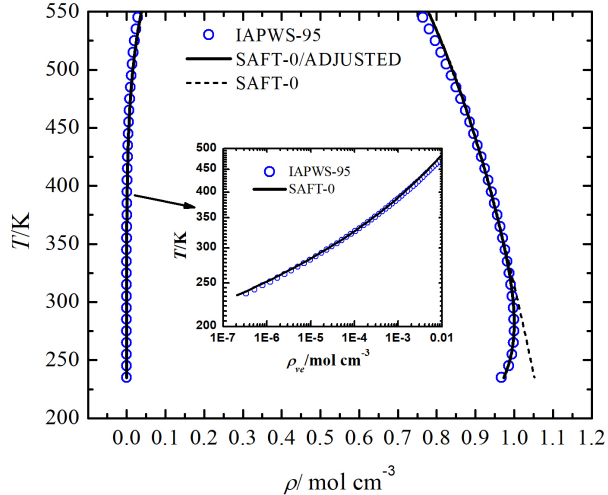


Figure 2: Binodal densities of water calculated using SAFT-0 and SAFT-0/ADJUSTED compared with IAPWS-95 values [49]. Inset: Log-Plot of saturated vapor density vs.  $T$ .

within the range of temperature  $220K - 445K$  very well with minor deviations near the range boundaries. However, one may reduce this deviation by calculating the fitting parameters of SAFT-0 EOS and the new parameter ( $\lambda$ ) within a shorter temperature range such as  $210K - 300K$ . In present work, we provide the acceptable fitting parameters in a very wide temperature range to make the adjusted SAFT-0 EOS ready for other studies.

Figure 3 compares accepted [49] binodal vapor densities and equilibrium vapor pressure of water with values calculated using the adjusted SAFT-0 EOS. We see the calculated results agree very well with experimental data in the temperature range  $235 - 450K$ , in particular the range relevant for nucleation measurements. The small deviation at very low temperature is due to the same reason mentioned above.

Both forms of the classical and nonclassical nucleation theories have been used with the SAFT-0 EOS to determine the nucleation rates of water. For comparison, Fig. 4 compares the predicted nucleation rates of water using the

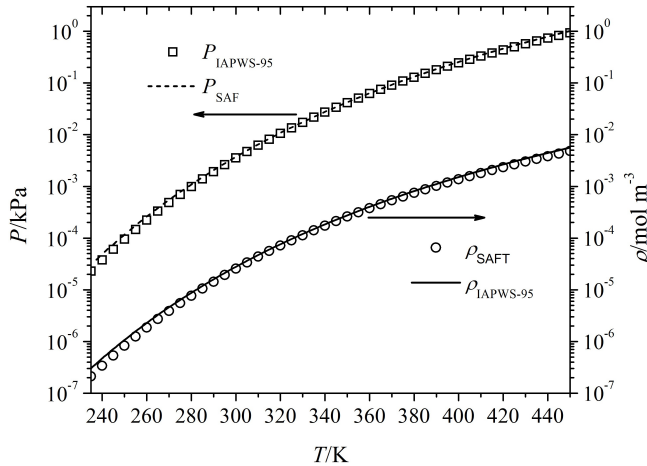


Figure 3: Log. plot of saturated vapor pressure  $P$  and density  $\rho$  of water calculated using  $T$ -adjusted SAFT-0 EOS compared with IAPWS-95 values [49].

SAFT-0 EOS in terms of Cotterman's form of  $d$  with Wölk and Strey measurements [20]. The reason for using Wölk and Strey measurements will be shown later below. We note that the GT and  $P$ -form roughly show a similar dependence on  $S$  ( $P$ -form has a slightly better slope at low temperatures), but the  $P$ -form has a better  $T$  dependence (the gaps between the experimental and predicted nucleation rates are smaller, particularly for small temperatures) and is about one order of magnitude higher than the GT. Neither GT nor CNT reproduces the  $J$  values very well.

We see in Fig. 5 that the nucleation rates using adjusted SAFT-0 EOS are considerably improved compared to the results in Fig. 4. First, the magnitudes of the nucleation rates are improved by factors of 500 and 100 for GT and CNT, respectively, but the  $P$ -form of CNT shows a slightly better  $S$  dependence. Second, we see that adjusting  $d$  by including the association energy significantly improves the  $T$  dependence of GT. Both the CNT and GT rates share the following features. At low temperatures in the figure 5, one sees poorer agreement with the data than at the higher temperatures because of the use of a constant scale factor.

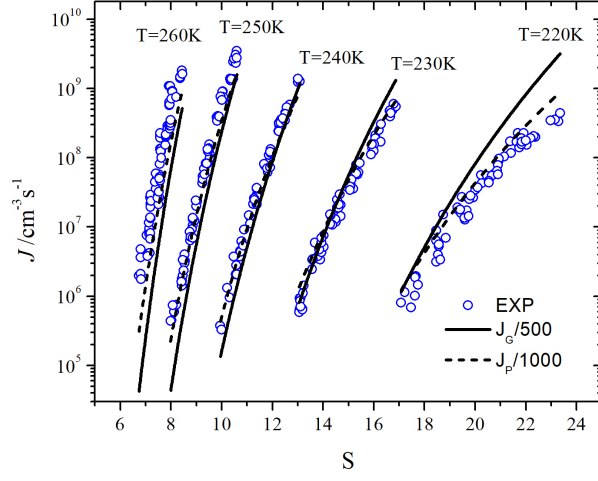


Figure 4: Nucleation rates of water using the SAFT-0 EOS with CNT and GT compared with experimental rates [20].  $J_G$ : gradient theory;  $J_P$ :  $P$ -form of CNT.

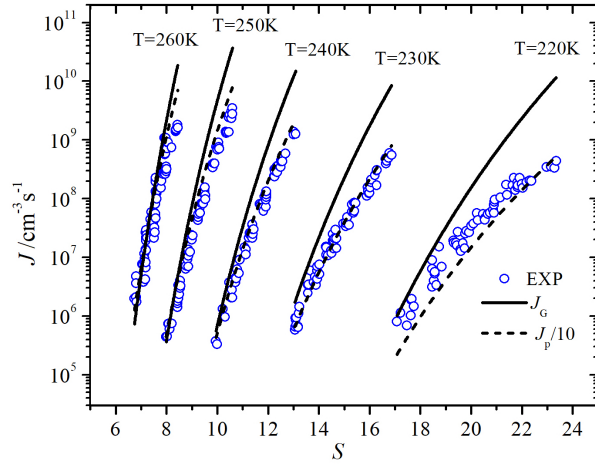


Figure 5: Nucleation rates of water using the adjusted SAFT-0 EOS with CNT and GT compared with experimental rates [20].  $J_G$ : gradient theory;  $J_P$ :  $P$ -form of CNT.

Next, we apply a  $T$ -dependent scaling factor and we discuss the  $T$  dependence of the rates in more detail. Since the GT calculations of nucleation rates of water are better by a factor of 10 than those from the P-form of CNT and because the GT usually gives better results for other associating compounds than the CNT[35], its predictions of nucleation rates will be assessed by Hale’s  $T$ -dependent scaling models [36, 76, 38, 37]. Hale’s scaled nucleation rate equation is, perhaps, the most useful semi-empirical model that accurately describes the temperature dependence for many simple vapor systems. It can be used to examine the accuracy of nucleation rate data. For example, Obeidat et al. [35] used Hale plot to assess Strey et al. [77, 78] measurements of methanol nucleation rates. Hale plots showed that the methanol rate data exhibit anomalous  $S - T$  dependence. Obeidat et al. attributed this to the inadequacy of the thermodynamic data base used by Strey et al. to correct the original  $S - T$  data for the effects of gas phase association.

Hale defined a simple scaled model of nucleation rate by exploiting scaled expressions for the vapor pressure and for the surface tensions[76, 79] as follows:

$$J_{scaled} = J_0 \exp \left[ -\frac{16\pi\Omega^3 \left(\frac{T_C}{T} - 1\right)^3}{3(\ln S)^2} \right], \quad (23)$$

where  $J_0$  is the kinetic prefactor for the steady state homogeneous nucleation rate,  $T_C = 647.15K$  is the experimental critical temperature of water, and  $\Omega = \sigma_0/k/\rho^{2/3}$  is the excess surface entropy per molecule estimated from the experimental values of surface tension (approximately 2 for normal liquids and 1.5 for polar substances). Here,  $\sigma_0$  is a material-dependent constant obtained by fitting the surface tension data as a linear equation of surface tension  $\gamma = \sigma_0(T_C - T)$ ,  $k$  is the Eotvos constant[80, 37], and  $\rho$  is the liquid number density. A comparison of the scaled model of nucleation rate with some experiments and GT is shown in Figure 6. Here, the experimental data and the GT predictions are plotted versus  $J_{scaled}(T_{exp}, S_{exp})$ , with  $\Omega = 1.45$ . The latter value of  $\Omega$  is in the expected range for polar substances (calculated by Hale et al.[76]). In addition to our calculated values of nucleation rates of water using GT, this comparison shows that Wök and Strey measurements scale very well and lie

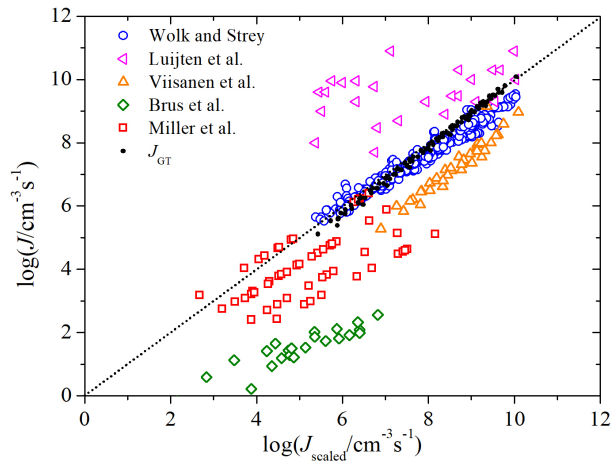


Figure 6: A comparison of the homogeneous nucleation rates of water predicted by Hale’s scaled model with several experimental data sets and our GT results, with  $\Omega = 1.45$ . The data sets are from the following references: Wölk and Strey[20], Luijten et al.[81], Viisanen et al.[82], Brus et al.[83], and Miller et al.[50]. The dotted line indicates perfect agreement.

along the perfect agreement line.

Hale’s plots provide a simple means of assessing the combined supersaturation and temperature dependence of a set of nucleation rates. For many systems, nucleation rate data from different laboratories often lie on or close to a single, universal line indicating mutual consistency [84, 85, 86, 87]. An application of the scaling that requires no knowledge of  $\Omega$  is shown in Figure 7 where  $\log J$  is plotted versus the scaled supersaturation ( $\ln S_{scaled} = \ln S / (T_c / T - 1)^{3/2}$ ) [37, 76]. The scaled supersaturation in Figure 7 is multiplied by a normalizing constant  $(T_c / 240 - 1)^{3/2}$ , so that the values fall in the same range as  $\ln S$ . Hence, the dashed line at  $T = 240K$  is the perfect agreement line. We see that the Wölk and Strey data corresponding to constant temperatures that spread out in the standard  $\log J_{exp}$  versus  $\ln S$  plot (indicated by the dot lines) collapse onto a single line (indicated by dashed line) when we plot  $\log J_{exp}$  versus  $\ln S_{scaled}$ . Similarly, the plot of  $\log J_{GT}$  versus  $\ln S_{scaled}$  shows a good scaling of the nucleation rates of water predicted by applying GT with adjusted SAFT-0 EOS (indicated with filled circles). As expected, the GT results scale

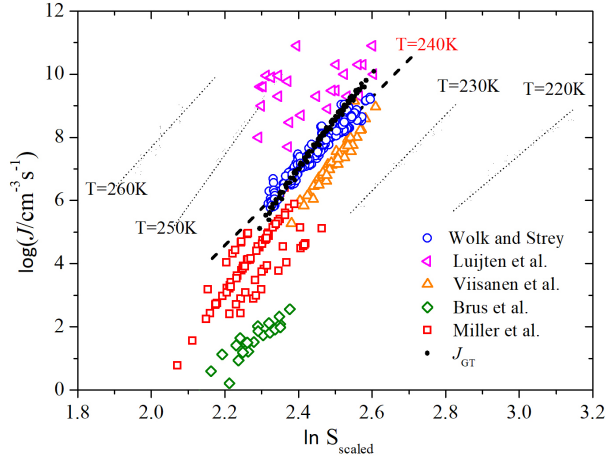


Figure 7: The GT predictions of homogeneous nucleation rates of water and experimental data plotted versus the scaled supersaturation function,  $\ln S/(T_c/T - 1)^{3/2}$ . The scaled supersaturation is multiplied by a normalizing constant,  $C_0 = (T_c/240 - 1)^{3/2}$ , so that the values fall in the same range of  $T = 240K$  (dashed line). The dotted lines indicate where the Wölk and Strey’s measurements fall if  $\log J_{exp}$  is plotted versus  $\ln S$  (before scaling  $S$ ). The references for the data are listed in the caption of Fig.6.

very well using Hale’s scaling model and show a good temperature-dependent agreement with the Wölk and Strey experimental data, but with slightly stronger dependence on the scaled supersaturation ratio (larger slope).

## 5. Conclusions

In order to solve the inaccuracy of SAFT-0 EOS in predicting the water binodal lines below  $T_{max}$ , we adjust the temperature-dependent hard sphere diameter by adding an exponential correction in terms of the association energy. The adjusted SAFT-0 EOS predicts the water phase equilibria adequately well within a temperature range of  $220K - 445K$ .

We have made classical and nonclassical nucleation rate calculations for water vapor using the SAFT-0 and adjusted SAFT-0 EOS. The calculated nucleation rates by GT and CNT are compared with Wölk and Strey measure-

ments [20] using a standard format. The adjusted SAFT-0 improves the GT and CNT calculations by factors of 500 and 100, respectively. Moreover, it significantly improves the  $T$  dependence of GT. Furthermore, both of the CNT and GT have a good  $S$  dependence at high temperatures while it is slightly better in CNT at low temperatures.

The GT results were compared with the experimental water data using the following Hale’s plots:  $\log J$  versus  $\log J_{scaled}$ , with  $\Omega = 1.45$ , and  $\log J$  versus  $\ln S_{scaled}$ , without assuming a value for  $\Omega$ . The calculations of GT and the measurements by Wölk and Strey scale remarkably well. The scaling of the GT rates is most likely due to the combination of a nonclassical nucleation theory that avoids the drastic and unphysical assumptions of CNT (incompressible bulk liquid with a sharp vapor-liquid interface [8, 30]) and an accurate equation of state (adjusted SAFT-0 EOS) that treats the effects of association. Also, we expect that one can significantly improve the calculations of water nucleation rates by applying gradient theory using our adjusted SAFT-0 EOS and WilhelmSEN et al. [23, 44] technique of including the curvature-dependence of surface tension.

We conclude that the adjusted SAFT-0 EOS is satisfactorily exact and predictive, thus future computational studies of more complex systems, such as aqueous-alcohol mixtures, are now expected to be more convenient and more accurate, in particular, below  $T_{max}$ .

## Acknowledgements

The author acknowledges Prof. Gerald Wilemski and Prof. Barbara Hale for valuable discussions and Dr. Abdalla Obeidat for sharing his GT code. He also acknowledges F. AlFaran and P. Field from HCT for their linguistic comments.

## References

## References

- [1] D. H. Rasmussen, M. T. Liang, E. Esen, M. R. Appleby, Nucleation in condensation, *Langmuir* 8 (7) (1992) 1868–1877. doi:[10.1021/la00043a030](https://doi.org/10.1021/la00043a030).
- [2] L. G. MacDowell, P. Virnau, M. Mller, K. Binder, The evaporation/condensation transition of liquid droplets, *J. Chem. Phys.* 120 (11) (2004) 5293–5308. doi:[10.1063/1.1645784](https://doi.org/10.1063/1.1645784).
- [3] A. Tabazadeh, Y. S. Djikaev, H. Reiss, Surface crystallization of supercooled water in clouds, *PNAS* 99 (25) (2002) 15873–15878. doi:[10.1073/pnas.252640699](https://doi.org/10.1073/pnas.252640699).
- [4] J. Hallett, Experimental studies of the crystallization of supercooled water, *Journal of the Atmospheric Sciences* 21 (6) (1964) 671–682. doi:[10.1175/1520-0469\(1964\)021<0671:ESOTC0>2.0.CO;2](https://doi.org/10.1175/1520-0469(1964)021<0671:ESOTC0>2.0.CO;2).
- [5] K.-i. Murata, H. Asakawa, K. Nagashima, Y. Furukawa, G. Sazaki, Thermodynamic origin of surface melting on ice crystals, *PNAS* 113 (44) (2016) E6741–E6748. doi:[10.1073/pnas.1608888113](https://doi.org/10.1073/pnas.1608888113).
- [6] J. Feder, K. C. Russell, J. Lothe, G. M. Pound, Homogeneous nucleation and growth of droplets in vapours, *Advances in Physics* 15 (57) (1966) 111–178. doi:[10.1080/00018736600101264](https://doi.org/10.1080/00018736600101264).
- [7] P. Rein ten Wolde, M. J. RuizMontero, D. Frenkel, Numerical calculation of the rate of crystal nucleation in a Lennard-Jones system at moderate undercooling, *J. Chem. Phys.* 104 (24) (1996) 9932–9947. doi:[10.1063/1.471721](https://doi.org/10.1063/1.471721).
- [8] J. W. Gibbs, *The Scientific Papers of J. W. Gibbs. Vo. 1*, Dover Publications, 1961.
- [9] M. Kulmala, P. E. Wagner, *Nucleation and Atmospheric Aerosols*, Elsevier, 1996.

- [10] A. W. Castleman, R. G. Keesee, Nucleation and Growth of Stratospheric Aerosols, *Annu. Rev. Earth Planet. Sci.* 9 (1) (1981) 227–249. doi:[10.1146/annurev.ea.09.050181.001303](https://doi.org/10.1146/annurev.ea.09.050181.001303).
- [11] D. V. Spracklen, K. S. Carslaw, M. Kulmala, V.-M. Kerminen, G. W. Mann, S.-L. Sihto, The contribution of boundary layer nucleation events to total particle concentrations on regional and global scales, *Atmospheric Chemistry and Physics* 6 (12) (2006) 5631–5648. doi:<https://doi.org/10.5194/acp-6-5631-2006>.
- [12] J. Curtius, Nucleation of atmospheric aerosol particles, *Comptes Rendus Physique* 7 (9) (2006) 1027–1045. doi:[10.1016/j.crhy.2006.10.018](https://doi.org/10.1016/j.crhy.2006.10.018).
- [13] Y. Viisanen, M. Kulmala, A. Laaksonen, Experiments on gas-liquid nucleation of sulfuric acid and water, *J. Chem. Phys.* 107 (3) (1997) 920–926. doi:[10.1063/1.474445](https://doi.org/10.1063/1.474445).
- [14] M. Volmer, A. Weber, Keimbildung in übersättigten Gebilden, *Z. phys. Chem* 119 (1926) 277–301.
- [15] L. Farkas, Keimbildungsgeschwindigkeit in übersättigten Dämpfen, *Zeitschrift für Physikalische Chemie* 125 (1) (1927) 236–242. doi:[10.1515/zpch-1927-12513](https://doi.org/10.1515/zpch-1927-12513).
- [16] R. Becker, W. Döring, Kinetische Behandlung der Keimbildung in übersättigten Dämpfen, *Annalen der Physik* 416 (8) (1935) 719–752. doi:[10.1002/andp.19354160806](https://doi.org/10.1002/andp.19354160806).
- [17] J. Frenkel, A General Theory of Heterophase Fluctuations and Pretransition Phenomena, *The Journal of Chemical Physics* 7 (7) (1939) 538–547. doi:[10.1063/1.1750484](https://doi.org/10.1063/1.1750484).
- [18] J. B. Zeldovich, Theory of the formation of a new phase, Cavitation., *Zh. Eksp. Teor. Fiz.* 12 (1942) 525 – 538.

- [19] S. Sinha, A. Bhabhe, H. Laksmono, J. Wölk, R. Strey, B. Wyslouzil, Argon nucleation in a cryogenic supersonic nozzle, *The Journal of Chemical Physics* 132 (6) (2010) 064304. doi:10.1063/1.3299273.
- [20] J. Wölk, R. Strey, Homogeneous Nucleation of H<sub>2</sub>O and D<sub>2</sub>O in Comparison: The Isotope Effect, *The Journal of Physical Chemistry B* 105 (47) (2001) 11683–11701. doi:10.1021/jp0115805.
- [21] D. Brus, V. Ždímal, J. Smolík, Homogeneous nucleation rate measurements in supersaturated water vapor, *The Journal of Chemical Physics* 129 (17) (2008) 174501. doi:10.1063/1.3000629.
- [22] D. W. Oxtoby, R. Evans, Nonclassical nucleation theory for the gas–liquid transition, *The Journal of Chemical Physics* 89 (12) (1988) 7521–7530. doi:10.1063/1.455285.
- [23] Ø. Wilhelmsen, T. T. Trinh, S. Kjelstrup, D. Bedeaux, Influence of Curvature on the Transfer Coefficients for Evaporation and Condensation of Lennard-Jones Fluid from Square-Gradient Theory and Nonequilibrium Molecular Dynamics, *J. Phys. Chem. C* 119 (15) (2015) 8160–8173. doi:10.1021/acs.jpcc.5b00615.
- [24] Ø. Wilhelmsen, D. Bedeaux, S. Kjelstrup, D. Reguera, Thermodynamic stability of nanosized multicomponent bubbles/droplets: The square gradient theory and the capillary approach, *J. Chem. Phys.* 140 (2) (2014) 024704. doi:10.1063/1.4860495.
- [25] J. S. Rowlinson, Translation of j. d. van der waals’ the thermodynamik theory of capillarity under the hypothesis of a continuous variation of density, *J. Stat. Phys.* 20 (2) (1979) 197–200.
- [26] J. W. Cahn, J. E. Hilliard, Free Energy of a Nonuniform System. III. Nucleation in a Two-Component Incompressible Fluid, *The Journal of Chemical Physics* 31 (3) (1959) 688–699. doi:10.1063/1.1730447.

- [27] D. Bedeaux, E. Johannessen, A. Rsjorde, The nonequilibrium van der Waals square gradient model. (I). The model and its numerical solution, *Physica A: Statistical Mechanics and its Applications* 330 (3) (2003) 329–353.
- [28] L. Grnsy, Nucleation theory for diffuse interfaces, *Materials Science and Engineering: A* 178 (1) (1994) 121–124. doi:[10.1016/0921-5093\(94\)90529-0](https://doi.org/10.1016/0921-5093(94)90529-0).
- [29] E. Johannessen, D. Bedeaux, The nonequilibrium van der Waals square gradient model. (III). Heat and mass transfer coefficients, *Physica A: Statistical Mechanics and its Applications* 336 (3) (2004) 252–270. doi:[10.1016/j.physa.2003.12.045](https://doi.org/10.1016/j.physa.2003.12.045).
- [30] A. Obeidat, J.-S. Li, G. Wilemski, Nucleation rates of water and heavy water using equations of state, *The Journal of Chemical Physics* 121 (19) (2004) 9510–9516. doi:[10.1063/1.1806400](https://doi.org/10.1063/1.1806400).
- [31] Z. Koiek, P. Demo, Size distribution of nuclei formed by homogeneous nucleation in closed systems, *Journal of Aerosol Science* 40 (1) (2009) 44–54. doi:[10.1016/j.jaerosci.2008.09.006](https://doi.org/10.1016/j.jaerosci.2008.09.006).
- [32] Z. Koek, P. Demo, Size distribution and growth rate of crystal nuclei near critical undercooling in small volumes, *IOP Conf. Ser.: Mater. Sci. Eng.* 266 (2017) 012006. doi:[10.1088/1757-899X/266/1/012006](https://doi.org/10.1088/1757-899X/266/1/012006).
- [33] W. G. Chapman, K. E. Gubbins, G. Jackson, M. Radosz, New reference equation of state for associating liquids, *Industrial & Engineering Chemistry Research* 29 (8) (1990) 1709–1721. doi:[10.1021/ie00104a021](https://doi.org/10.1021/ie00104a021).
- [34] A. Obeidat, G. Wilemski, Gradient theory of nucleation in polar fluids, *Atmospheric Research* 82 (3–4) (2006) 481–488. doi:[10.1016/j.atmosres.2006.02.005](https://doi.org/10.1016/j.atmosres.2006.02.005).
- [35] A. Obeidat, M. Gharaibeh, H. Ghanem, F. Hrahsheh, N. Al-Zoubi, G. Wilemski, Nucleation Rates of Methanol Using the SAFT-0 Equation

- of State, ChemPhysChem 11 (18) (2010) 3987–3995. doi:10.1002/cphc.201000493.
- [36] B. N. Hale, Temperature dependence of homogeneous nucleation rates for water: Near equivalence of the empirical fit of Wölk and Strey, and the scaled nucleation model, The Journal of Chemical Physics 122 (20) (2005) 204509. doi:10.1063/1.1906213.
- [37] B. N. Hale, Application of a scaled homogeneous nucleation-rate formalism to experimental data at  $T \ll T_C$ , Physical Review A 33 (6) (1986) 4156–4163. doi:10.1103/PhysRevA.33.4156.
- [38] B. N. Hale, The scaling of nucleation rates, Metallurgical Transactions A 23 (7) (1992) 1863–1868. doi:10.1007/BF02647536.
- [39] H. Vehkamäki, Classical Nucleation Theory in Multicomponent Systems, Springer-Verlag, 2006.
- [40] P. G. Debenedetti, Metastable Liquids: Concepts and Principles, Princeton University Press, 1996.
- [41] V. Kalikmanov, Nucleation Theory, Vol. 860, Springer Netherlands, 2013. doi:10.1007/978-90-481-3643-8.
- [42] D. Kashchiev, Nucleation: Basic Theory with Applications, Butterworth Heinemann, 2000.
- [43] K. Iland, J. Wlk, R. Strey, D. Kashchiev, Argon nucleation in a cryogenic nucleation pulse chamber, J. Chem. Phys. 127 (15) (2007) 154506. doi:10.1063/1.2764486.
- [44] Ø. Wilhelmsen, D. Bedeaux, D. Reguera, Communication: Tolman length and rigidity constants of water and their role in nucleation, J. Chem. Phys. 142 (17) (2015) 171103. doi:10.1063/1.4919689.
- [45] G. M. Kontogeorgis, M. L. Michelsen, G. K. Folas, S. Derawi, N. von Solms, E. H. Stenby, Ten Years with the CPA (Cubic-Plus-Association) Equation

- of State. Part 1. Pure Compounds and Self-Associating Systems, *Ind. Eng. Chem. Res.* 45 (14) (2006) 4855–4868. doi:10.1021/ie051305v.
- [46] M. L. Michelsen, E. M. Hendriks, Physical properties from association models, *Fluid Phase Equilibria* 180 (1) (2001) 165–174. doi:10.1016/S0378-3812(01)00344-2.
- [47] W. Helfrich, Elastic Properties of Lipid Bilayers: Theory and Possible Experiments, *Z. Naturforsch. C* 28 (11-12) (1973) 693–703. doi:10.1515/znc-1973-11-1209.
- [48] P. Guo, H. Tu, Z. Wang, Q. Wang, Calculation of thermodynamic properties of water by the CPA equation of state, *Natural Gas Industry B* 4 (4) (2017) 305–310. doi:10.1016/j.ngib.2017.08.014.
- [49] W. Wagner, A. Pruß, The IAPWS Formulation 1995 for the Thermodynamic Properties of Ordinary Water Substance for General and Scientific Use, *Journal of Physical and Chemical Reference Data* 31 (2) (2002) 387–535. doi:10.1063/1.1461829.
- [50] R. C. Miller, R. J. Anderson, J. L. Kassner, D. E. Hagen, Homogeneous nucleation rate measurements for water over a wide range of temperature and nucleation rate, *The Journal of Chemical Physics* 78 (6) (1983) 3204–3211. doi:10.1063/1.445236.
- [51] J.-S. Li, G. Wilemski, Temperature dependence of droplet nucleation in a Yukawa fluid, *The Journal of Chemical Physics* 118 (6) (2003) 2845–2852. doi:10.1063/1.1534830.
- [52] A. Obeidat, Nucleation theory using equations of state, Ph. D. Thesis, University of Missouri-Rolla, 2003.
- [53] M. S. Wertheim, Fluids with highly directional attractive forces. I. Statistical thermodynamics, *Journal of Statistical Physics* 35 (1-2) (1984) 19–34. doi:10.1007/BF01017362.

- [54] A. Gil-Villegas, A. Galindo, P. J. Whitehead, S. J. Mills, G. Jackson, A. N. Burgess, Statistical associating fluid theory for chain molecules with attractive potentials of variable range, *J. Chem. Phys.* 106 (10) (1997) 4168–4186. doi:10.1063/1.473101.
- [55] J. Gross, G. Sadowski, Application of the Perturbed-Chain SAFT Equation of State to Associating Systems, *Ind. Eng. Chem. Res.* 41 (22) (2002) 5510–5515. doi:10.1021/ie010954d.
- [56] F. Llovel, L. F. Vega, Prediction of Thermodynamic Derivative Properties of Pure Fluids through the Soft-SAFT Equation of State, *J. Phys. Chem. B* 110 (23) (2006) 11427–11437. doi:10.1021/jp0608022.
- [57] S. P. Tan, H. Adidharma, M. Radosz, Recent Advances and Applications of Statistical Associating Fluid Theory, *Industrial & Engineering Chemistry Research* 47 (21) (2008) 8063–8082. doi:10.1021/ie8008764.
- [58] S. J. Suresh, J. R. Elliott, Multiphase equilibrium analysis via a generalized equation of state for associating mixtures, *Industrial & Engineering Chemistry Research* 31 (12) (1992) 2783–2794. doi:10.1021/ie00012a025.
- [59] M. S. Wertheim, Fluids with highly directional attractive forces. II. Thermodynamic perturbation theory and integral equations, *Journal of Statistical Physics* 35 (1-2) (1984) 35–47. doi:10.1007/BF01017363.
- [60] J. A. Barker, D. Henderson, Perturbation Theory and Equation of State for Fluids. II. A Successful Theory of Liquids, *The Journal of Chemical Physics* 47 (11) (1967) 4714–4721. doi:10.1063/1.1701689.
- [61] R. L. Cotterman B. J. Schwarz J. M. Prausnitz, Molecular thermodynamics for fluids at low and high densities part i: Pure fluids containing small or large molecules., *AIChE J.* 32 (1986) 1787–1798.
- [62] R. Ludwig, Water: From Clusters to the Bulk, *Angewandte Chemie International Edition* 40 (10) (2001) 1808–1827. doi:10.1002/1521-3773(20010518)40:10<1808::AID-ANIE1808>3.0.CO;2-1.

- [63] J. K. Gregory, D. C. Clary, K. Liu, M. G. Brown, R. J. Saykally, The Water Dipole Moment in Water Clusters, *Science* 275 (5301) (1997) 814–817. [arXiv:9012344](https://arxiv.org/abs/9012344), [doi:10.1126/science.275.5301.814](https://doi.org/10.1126/science.275.5301.814).
- [64] D. D. Kemp, M. S. Gordon, An Interpretation of the Enhancement of the Water Dipole Moment Due to the Presence of Other Water Molecules, *J. Phys. Chem. A* 112 (22) (2008) 4885–4894. [doi:10.1021/jp801921f](https://doi.org/10.1021/jp801921f).
- [65] B. D. Marshall, On the cooperativity of association and reference energy scales in thermodynamic perturbation theory, *J. Chem. Phys.* 145 (20) (2016) 204104. [doi:10.1063/1.4967966](https://doi.org/10.1063/1.4967966).
- [66] B. D. Marshall, A second order thermodynamic perturbation theory for hydrogen bond cooperativity in water, *J. Chem. Phys.* 146 (17) (2017) 174104. [doi:10.1063/1.4982229](https://doi.org/10.1063/1.4982229).
- [67] C. Held, L. F. Cameretti, G. Sadowski, Modeling aqueous electrolyte solutions: Part 1. Fully dissociated electrolytes, *Fluid Phase Equilibria* 270 (1) (2008) 87–96. [doi:10.1016/j.fluid.2008.06.010](https://doi.org/10.1016/j.fluid.2008.06.010).
- [68] L. F. Cameretti, G. Sadowski, J. M. Mollerup, Modeling of Aqueous Electrolyte Solutions with Perturbed-Chain Statistical Associated Fluid Theory, *Ind. Eng. Chem. Res.* 44 (9) (2005) 3355–3362. [doi:10.1021/ie0488142](https://doi.org/10.1021/ie0488142).
- [69] L. F. Cameretti, *Modeling of Thermodynamic Properties in Biological Solutions*, Cuvillier Verlag, 2009.
- [70] S. S. Chen and A. Kreglewski, Applications of the augmented van der waals theory of fluids. i. pure fluids, *Ber. Bunsen-Ges. Phys. Chem.* 81 (1977) 1048–1052.
- [71] J. A. Barker and D. J. Henderson, Perturbation theory and equation of state for fluids. ii. a successful theory of liquids, *J. Chem. Phys.* 47 (1967) 4714–4721.

- [72] S. Pereda, J. A. Awan, A. H. Mohammadi, A. Valtz, C. Coquelet, E. A. Brignole, D. Richon, Solubility of hydrocarbons in water: Experimental measurements and modeling using a group contribution with association equation of state (GCA-EoS), *Fluid Phase Equilibria* 275 (1) (2009) 52–59. doi:[10.1016/j.fluid.2008.09.008](https://doi.org/10.1016/j.fluid.2008.09.008).
- [73] M. S. Zabaloy, G. D. B. Mabe, S. B. Bottini, E. A. Brignole, Vapor liquid equilibria in ternary mixtures of water-alcohol-non polar gases, *Fluid Phase Equilibria* 83 (1993) 159–166. doi:[10.1016/0378-3812\(93\)87018-V](https://doi.org/10.1016/0378-3812(93)87018-V).
- [74] H. P. Gros, S. Bottini, E. A. Brignole, A group contribution equation of state for associating mixtures, *Fluid Phase Equilibria* 116 (1) (1996) 537–544. doi:[10.1016/0378-3812\(95\)02928-1](https://doi.org/10.1016/0378-3812(95)02928-1).
- [75] F. Mallamace, C. Branca, M. Broccio, C. Corsaro, C.-Y. Mou, S.-H. Chen, The anomalous behavior of the density of water in the range  $30\text{ K} < T < 373\text{ K}$ , *Proceedings of the National Academy of Sciences* 104 (47) (2007) 18387–18391. arXiv:<https://www.pnas.org/content/104/47/18387.full.pdf>, doi:[10.1073/pnas.0706504104](https://doi.org/10.1073/pnas.0706504104).
- [76] B. N. Hale, D. J. DiMattio, Scaling of the Nucleation Rate and a Monte Carlo Discrete Sum Approach to Water Cluster Free Energies of Formation, *The Journal of Physical Chemistry B* 108 (51) (2004) 19780–19785. doi:[10.1021/jp0476343](https://doi.org/10.1021/jp0476343).
- [77] R. Strey, P. E. Wagner, T. Schmeling, Homogeneous nucleation rates for n-alcohol vapors measured in a two-piston expansion chamber, *The Journal of Chemical Physics* 84 (4) (1986) 2325–2335. doi:[10.1063/1.450396](https://doi.org/10.1063/1.450396).
- [78] R. Strey, T. Schmeling, P. E. Wagner, The effect of the heat of association on homogeneous nucleation rates in methanol vapor, *The Journal of Chemical Physics* 85 (10) (1986) 6192–6196. doi:[10.1063/1.451486](https://doi.org/10.1063/1.451486).
- [79] B. N. Hale, The scaling of nucleation rates, *Metallurgical Transactions A* 23 (1973) 1863–1868. doi:[10.1007/BF02647536](https://doi.org/10.1007/BF02647536).

- [80] F. H. MacDougall, *Physical Chemistry*, Macmillan, New York, 1936.
- [81] C. C. M. Luijten, K. J. Bosschaart, V. M. E.H. Dongen, High pressure nucleation in water/nitrogen systems, *Journal of Chemical Physics* 106 (19) (1997) 8116–8123. doi:10.1063/1.473818.
- [82] Y. Viisanen, R. Strey, H. Reiss, Homogeneous nucleation rates for water, *The Journal of Chemical Physics* 99 (6) (1993) 4680–4692. doi:10.1063/1.466066.
- [83] D. Brus, V. dmal, J. Smolk, Homogeneous nucleation rate measurements in supersaturated water vapor, *The Journal of Chemical Physics* 129 (17) (2008) 174501. doi:10.1063/1.3000629.
- [84] M. Gharibeh, Y. Kim, U. Dieregswiler, B. E. Wyslouzil, D. Ghosh, R. Strey, Homogeneous nucleation of n-propanol, n-butanol, and n-pentanol in a supersonic nozzle, *The Journal of Chemical Physics* 122 (9) (2005) 094512. doi:10.1063/1.1858438.
- [85] D. Brus, V. Ždímal, F. Stratmann, Homogeneous nucleation rate measurements of 1-propanol in helium: The effect of carrier gas pressure, *The Journal of Chemical Physics* 124 (16) (2006) 164306. doi:10.1063/1.2185634.
- [86] D. Ghosh, A. Manka, R. Strey, S. Seifert, R. E. Winans, B. E. Wyslouzil, Using small angle x-ray scattering to measure the homogeneous nucleation rates of n-propanol, n-butanol, and n-pentanol in supersonic nozzle expansions, *The Journal of Chemical Physics* 129 (12) (2008) 124302. doi:10.1063/1.2978384.
- [87] D. Ghosh, D. Bergmann, R. Schwering, J. Wölk, R. Strey, S. Tanimura, B. E. Wyslouzil, Homogeneous nucleation of a homologous series of n-alkanes ( $C_iH_{2i+2}$ ,  $i=7-10$ ) in a supersonic nozzle, *The Journal of Chemical Physics* 132 (2) (2010) 024307. doi:10.1063/1.3274629.